Chapter 6

Differences in atmospheric boundary layer characteristics between an inland and a coastal region over southeast India

6.1. Introduction

The structure and evolution of the ABL depends primarily on earth's surface through sensible heat flux. Several other forcing factors also affect the ABL, including synoptic scale flows, entrainment flux from the top of ABL, descending motion in high-pressure systems, etc. (*Barlow et al., 2011; Bianco et al., 2010*; references therein). A sound understanding of the impact of such processes on ABL and its evolution is important for several reasons, for example assessment of air quality, improved weather forecasting and climate studies (*Monks et al., 2009; Gerbig et al., 2008*). Nevertheless, none of the above forcings (excluding sensible heat flux) can uniquely and solely define the evolution of ABL, rather they dominate in a certain situation (time of the day or geographical location). As seen in Chapter 4, the entrainment flux becomes important during the evening, when the sensible flux starts diminishing. There also exist a few additional forcing factors that have a strong control over the ABL near the mountainous and coastal regions. These meso-scale flows, such as land-sea breezes near the coastal regions and mountain-valley winds in mountainous regions, at times become too strong and affect the ABL dramatically. Therefore, one can expect the ABL to be quite different in regions dominated by the meso-scale flows, like inland and coastal regions.

Extensive literature is available on the structure and dynamics of ABL in last few decades using in situ and remote sensing instruments over different surfaces. For instance, over the land, the growth of ABL is controlled by several factors, such as surface conditions that includes soil type and quantity of soil moisture (Chapter 3), entrainment flux (Chapter 4), and local and synoptic circulations (*Barlow et al., 2011*). In addition to the above factors, ABL is largely influenced by local breeze circulations and coastal shape along the coastal region (*Aggarwal et al., 1980; Raghukumar et al., 1986; Prakash et al., 1992; Melas et al., 2000; Srinivas et al., 2006; Lemonsu et al., 2006; Talbot et al., 2007*). The coastal ABL (here after referred to as CoABL) is a transition zone in which airflow constantly adjusts to the new boundary conditions when it crosses shoreline. Several studies focused on the diurnal evolution of CoABL because of its role in regulating the extent of pollution dispersion and transport of fluxes (*Angevine et al., 2004; Docera et al., 2007*; *Levi et al., 2011; Munoz et al., 2011; Haman et al., 2012; May et al., 2012; Pena et al., 2013; Pandolfi et al., 2013; Banks et al., 2015). Kossmann et al. (2002)* observed interacting multi-scale wind systems ranging from micro-scale slope winds to meso-scale coast-to-basin flows that have an impact on the temporal and spatial variation of the ABL.

Despite this impressive body of work, many challenges yet remain in describing and understanding the CoABL.

The differences in ABL characteristics between land and coastal stations have been studied extensively using observations and models in different parts of the world. *Kara and Elsner (1998)* examined the characteristics of ABL (ABL height, friction velocity, Monin-Obukhov length) over coastal and inland stations in the United States of America during a single return flow current. The ABL is found to be shallower over coastal stations than that of inland and it is mainly due to the incursion of sea-breeze flow (*Lieman and Alpert 1993*) into the land region. They also infer the effect of sea-breeze circulation on ABL height and on dispersion of pollutants. Using radiosonde measurements, the spatial variability of the ABL characteristics (winds, turbulence, potential temperature, mixing ratio) have been studied over eastern equatorial Pacific and Israel, respectively, by *Yin and Albrecht (2000)* and *Dayan et al. (2002). Luo et al. (2014),* analyzed the diurnal and seasonal cycles of ABL height and its vertical structure over the ocean and land using the radiosonde and micro-pulse lidar measurements. Recently, *Sastre et al. (2015)* performed a comparison between ABL transitions at two experimental sites (France and Spain) by employing two intense field campaign observations, CIBA and BLLAST. They analysed the evolution of several variables during the evening transition. A common pattern is noticed in the evolution of TKE and $\Delta\Theta/\Delta z$ at both coastal and inland stations but there is a time lag in turbulence decay and katabatic occurrence (less frequent events and more intense at driest site). At the driest site, the crossover of the sensible heat flux takes place later. Water vapor at the surface and aloft and soil moisture are found to have crucial importance explaining most of the site-to-site differences (*Sastre et al., 2015*).

There were some efforts to understand the characteristics of ABL at Indian coastal and land stations using mostly radiosonde observations and models (*Holt and Sethuraman, 1986; Rao and Sethuraman, 1991; Gera et al., 1998; Rao and Murthy, 2001; Parameswaran et al., 2001b; Prabha et al., 2002; Jamima and Lakshminarasimhan, 2004; Sam et al., 2007; Sandhya et al., 2011*). Intense field campaigns, like MONTBLEX and BOBMEX, were conducted to understand the ABL variations over different surface conditions (*Goel and Srivastava, 1990; Murthy et al., 1996; Bhat et al , 2002*). Using a suite of instruments at Gadanki, including in situ and remote sensing, *Mohan and Rao (2012)* studied intriguing differences in ABL characteristics (CAPE, temperature, humidity, ABL height, evolution and low-level jet) between two

contrasting spells of Indian summer monsoon over southeast India. They noticed that the maximum differences in temperature, humidity and diurnal amplitude of LLJ between the spells occur within the ABL.

While basic understanding of the structure of ABL at inland and coastal regions has improved mostly based on the radiosonde observations, it is not clear whether or not the recent intriguing observations made at land-locked stations, like Gadanki, are global in nature or localized? For instance, the differences in the evolution of ABL (Chapter 3), top-to-bottom evolution of afternoon transition (Chapter 4) and frequent occurrence of PST and its height variation (Chapter 5). Moreover, most of the above studies that dealt the spatial variations in ABL were based on limited observations. A comprehensive study describing the variability of ABL and its state variables from the coast to inland has not been studied due to lack of suitable measurements. In this regard, there are some key questions that need to be answered. 1) How different is the evolution of ABL over the two observational sites (land and coastal)? What are the physical mechanisms that alter the evolution at these two sites? 2) How different are afternoon transitions in the coastal and inland regions? 3) What is the impact of sea-breeze circulation on the observed ABL characteristics over a coastal region? 4) Does PST occur over a coastal station? If so, how different is it from that of over an inland station? Therefore, the main objective of this chapter is to understand the similarities and differences in ABL characteristics (evolution of ABL, transitions, PST, etc.) between two contrasting experimental sites that are influenced by significantly different forcing factors due to heterogeneity in terrain characteristics and canopy and meso-scale flows.

The structure of the present chapter is as follows: Section 6.2 introduces the data and the instrumentation employed in the present chapter. Differences in the evolution of the ABL and its characteristics (ABL height, winds and turbulence) between inland and coastal regions have been studied in section 6.3. The afternoon transitions over inland and coastal regions are compared and contrasted in section 6.4. The occurrence statistics of PST and the major differences in the intensity of turbulence and radar echo characteristics over inland and coastal regions are studied in section 6.5. The results are summarized in section 6.6.

6.2. Data and instrumentation

The two stations chosen for the experiment are Gadanki and Kalpakkam (coastal station). Gadanki, an inland station, is surrounded by mountains of varying heights from 200-1000 m and nearly 90 km away from the coast. The terrain around Kalpakkam, a coastal station, is flat and the coast is just 5 km away from the chosen experimental site. The breeze circulations are frequently observed over Kalpakkam region due to land-sea temperature contrast and the Thermal Internal Boundary Layer (TIBL) also exist up to 100-200 m (*Prabha et al., 2002*). Though NARL is well equipped with all instrumentation required for ABL studies, only flux measurements were available at Kalpakkam. To obtain continuous wind and turbulence information, an UHF profiler, similar to that of at NARL, was installed at Kalpakkam. These two wind profiling radars (WPR), operating in UHF band, were developed indigenously at NARL. The profiler at Gadanki is fixed and referred to here as WPR_{16x16} and the profiler installed at Kalpakkam is a portable system and referred to here as WPR_{8X8} Complete details about both the systems are given in Chapter 2. Along with UHF wind profilers, both stations had micrometeorological towers with sensors at different levels on the tower. In addition, both stations had sensors for incoming shortwave radiation (Pyranometer) at 1.2 m level and soil moisture (soil moisture probe PR 2/6) at 6 levels (10, 20, 30, 40, 60 and 100 cm) at Gadanki and at 4 levels (30, 60, 90, 120 cm) at Kalpakkam.

At both stations, the WPRs are operated in two different modes (low and high) with each mode having 5-beams (see Table 6.1) to obtain the radar attributes (SNR, σ, 3D winds) at ~6 min temporal and 150 m range resolutions. Owing to higher sensitivity of these radars to precipitation, the backscattered echo comprises information of precipitation, but not ambient air. Therefore, only fair weather days were selected using incoming shortwave radiation measurements from Pyranometer. A total of 112 and 98 days of wind profiler data were available for further processing at Gadanki and Kalpakkam, respectively from the campaign period (September 2010-February 2011). After scrutinizing the range-time plots of spectral moments (SNR, w and σ) for clear growth and decay of the ABL and convection/precipitation contamination (*Grimsdell et al., 2002; Rao et al., 2008b*), 53 and 69 days of quality data were selected for Gadanki and Kalpakkam regions. We utilized these measurements to examine the characteristics of ABL between an inland and a coastal region. The procedures described in

chapters 4 and 5 are followed for the identification of the start of AT and PST, respectively. Special emphasis has been given to the mean characteristics of AT and PST.

Table 6.1: Experimental specification files of WPR_{16x16} (Gadanki) and WPR_{8x8} (Kalpakkam).

Parameter	WPR_{16x16}	WPR_{8x8}
Location	Gadanki	Kalpakkam
Coherent integrations	32	32
FFT points	1024	1024
Incoherent integrations	20	20
Pulse width (μs)	4	0.5
Coded/uncoded	Coded (4 bits)	Uncoded
Interpulse period (μs)	50	55
Range resolution (m)	150	75
Minimum height (km)	0.9	0.3
Maximum height (km)	6	7.725
Beam positions	E15, W15, Zx, N15, S15	E20, W20, Zx, N20, S20
Data period	October 2010-February 2011	

6.3. Differences in the ABL evolution between inland and coastal stations

The similarities and differences in the evolution of the ABL between two diverse regions of southeast India have been discussed in detail first through typical case studies and later making use of total data. For the case study, measurements from 07-09 February 2011 at Gadanki and 05-07 February 2011 at Kalpakkam have been used for a detailed study.

6.3.1. A case study

Figures 6.1 and 6.2 show the range-time intensity of radar attributes (range-corrected-SNR (hereafter simply referred to as SNR), σ, w, wind speed (ws) and wind direction (wd)) during 07-09 February 2011 and 05-07 February 2011, depicting the diurnal variation of the ABL at an inland and coastal stations, respectively. Hereafter, unless stated the given height is above the ground level.

The height of the ABL (stars on Figures 6.1a and 6.2a) is obtained from wind profiler observations using many parameters (SNR, σ and w variance) through fuzzy-logic method, following *Bianco et al. (2008)*. Figure 6.1 clearly resembles the growth of the Inland ABL on all days, presents the higher SNR values (day-to-day variability). Such ABL growth is a four phase process. In phase 1, the ABL growth is shallow from 0.6 to 0.9 km during ~08-09 LT and usually depends upon the availability of incoming solar radiation on the surface. In phase 2, once the cool nocturnal air is warmed, the ABL reaches to the base of the residual layer (~1 km in this case). In phase 3, the growth of the ABL becomes rapid and reaches up to the level of capping inversion (~2.1 km in this case on all 3 days). During this phase, the overshooting convective air motions (Figure 6.1c) will be replaced by entraining free atmospheric drier air and such intense up-and-downdrafts generates strong turbulence (Figure 6.1b shows larger σ values). Furthermore, the growth of the ABL is relatively constant at the level of capping inversion (but small fluctuations may arise due to balance between the entrainment flux, advection with buoyancy) and is called semi-stagnant phase (1.8-2.1 km in this case). In phase 4, the ABL begins to descent/fall down because of the weakening thermals (*Nieuwstadt and Brost, 1986*) and reaches a minimum value by evening.

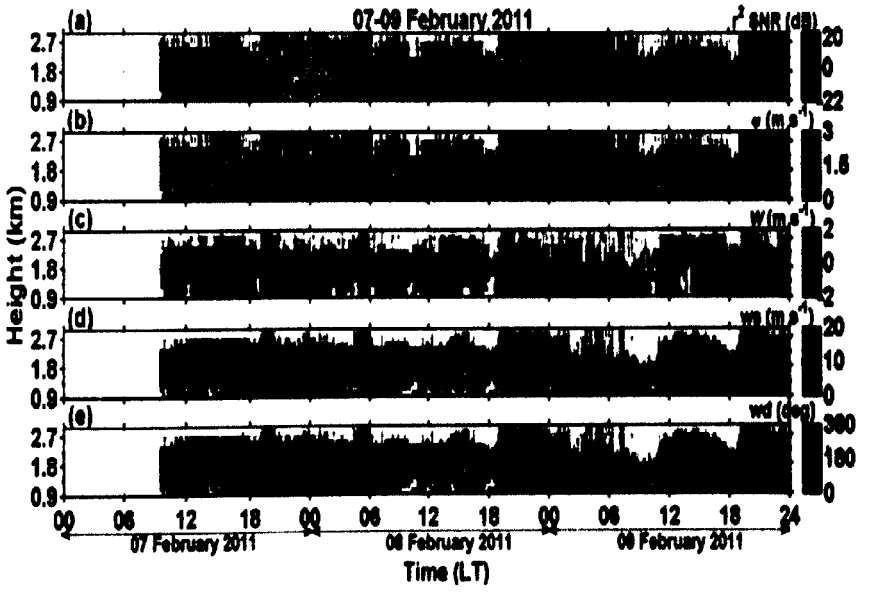

Figure 6.1: Time-height (a.g.l) variation of WPR attributes ((a) range-corrected SNR, (b) spectral width, (c) vertical air motion, (d) wind speed and (e) wind direction) during 07-09 February 2011, depicting the evolution of the ABL at an inland station. The solid stars on (a) represent the height of ABL.

The decay phase of the ABL is not so clear compared to the growth phase of the ABL (Figure 6.1). Figure 6.1c depicts the strength of the active thermals, which are in the range of ±2 m s^{-1} during the daytime and weakens during the initial phase of AT. Nevertheless, larger values of SNR (Figure 6.1a) and σ (Figure 6.1b) are observed after the sunset up to greater altitudes and the strength is almost equal or higher to that of during the day time, when thermals are buoyantly active. In fact, these PSTs are present on all the days with varying persistent periods. For instance, the PST varies quite dramatically both in height and intensity on 07 February 2011 and present throughout the night, whereas on other two days, PST persists only till mid-night.

Figure 6.2 clearly resembles the typical evolution of the ABL over a coastal region. The four phases described above over Gadanki, do present (but with large day-to-day variability) even at the coastal station. The evolution of the ABL is also clearly apparent, i.e. enhanced SNR and σ during the growth phase with strong thermals reaching up to ABL top. Several other similarities also exist in the characteristics of ABL over inland and coastal stations. The diurnal evolution is more prominent during the growth phase than decay phase. Larger values of SNR and σ up to greater altitudes are observed during the post-sunset period in both regions but the intensity of PST appears to be less over Kalpakkam.

Distinguishable differences in the ABL also exist between an inland and a coastal station, amidst 1) the ABL is deeper over an inland station, where it rises up to an altitude of 1.8-2.1 km, than over the coastal station (1.5-1.8 km). 2) The rapid growth of the ABL is delayed by 1-2 h on all days over a coastal station (The ABL growth (stars on SNR plots - Figures 6.1a and 6.2a) typically starts at ~08 LT over Gadanki, but it starts at ~09-10 LT over Kalpakkam). 3) It is also observed that the ABL grows to its maximum height at different timings at Gadanki and Kalpakkam, i.e., to 2.1 km during 14-15 LT over Gadanki and to 1.8 km during 11-12 LT over Kalpakkam. 5) The magnitude of SNR (σ) is much larger (smaller) at Kalpakkam than at Gadanki in the lower part of ABL during the day.

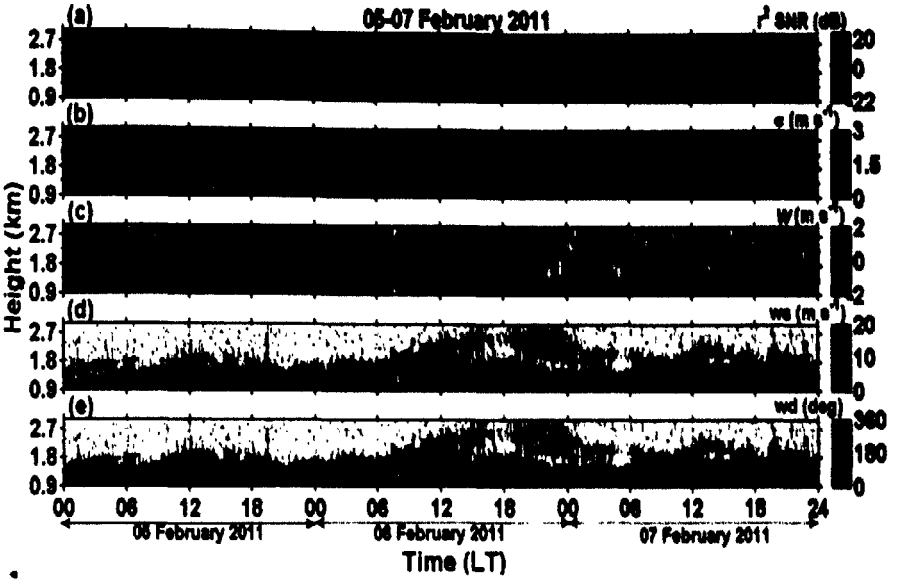

Figure 6.2: Same as Figure 6.1, but for 05-07 February 2011, depicting the evolution of the ABL over a coastal station.

Though the case study presented for Kalpakkam is typical and truly represents the coastal ABL variation in the absence of strong sea-breeze. However, the ABL variation and its evolution differ completely from that depicted in Figure 6.2 on strong sea-breeze days. After the intrusion of sea-breeze, discerning ABL height and other characteristics becomes difficult. Strong see-breezes were observed on some days during the campaign period, mostly in the early period of the campaign. Strong see-breeze occurs due to the differential heating between the sea and land. Since 95% of the campaign falls in post-monsoon and winter seasons, such large differential heating (and strong sea-breezes) does not exist. Moreover, it is easy to discern the sea-breeze during the monsoon season, because both synoptic monsoon flow (westerly) and sea-breeze (easterly) flow are in opposite direction. During post-monsoon and winter, the sea-breeze flow (easterly) is nearly in the direction of the synoptic flow (northeasterly-easterly). Therefore, the ABL characteristics associated with strong sea-breeze days were not presented here.

6.3.2. Mean characteristics of the ABL between inland and coastal stations

This section presents mean characteristics of the ABL (height of ABL, winds, turbulence) over inland and coastal stations with a special emphasis on the evolution of the ABL. It also

discusses the responsible factors for the observed differences in the evolution between the stations. From hourly radar attributes, ABL height is estimated following *Bianco et al. (2008)*. As noted in case studies, growth phase of the ABL is well defined and therefore identification of ABL height is straightforward. On the other hand, the ABL height is ill-defined and less discernible on many days during the decay period and such cases are omitted from the present study. As a result, the number of hourly data points (of ABL height) reduces during the afternoon period (not shown).

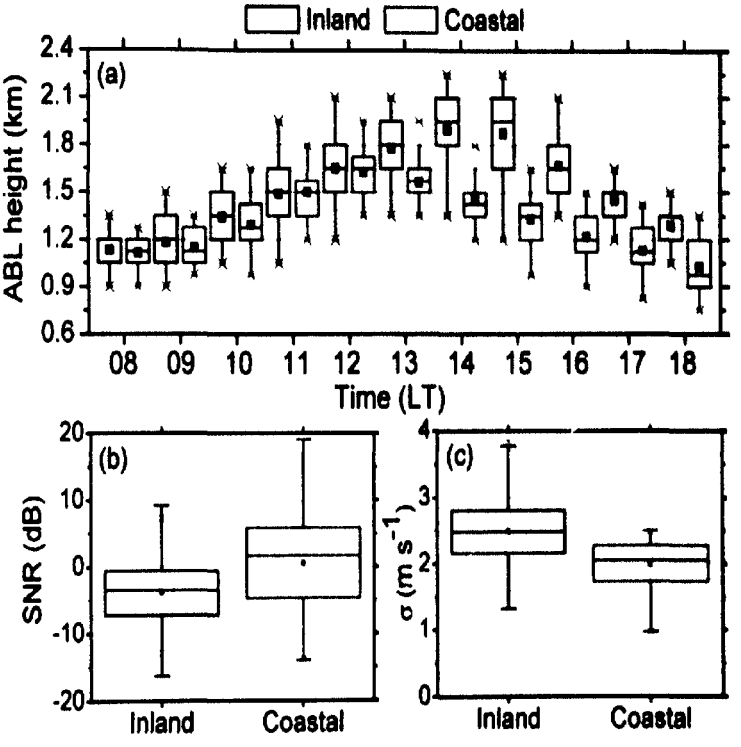

Figure 6.3: Temporal variation of the distribution of (a) mean ABL height at inland (blue) and coastal (red) station. Boxplots of (b) SNR (c) σ during th afternoon period (11-13 LT) below 1.5 km. The mean is taken over 53 (69) inland (coastal) days.

The day-time diurnal cycle of the mean ABL height over the two stations is presented in Figure 6.3 to understand the major differences between the stations. The important differences, among others, are briefed here. 1) Both inland and coastal stations reveal a strong diurnal cycle in the ABL height, with a distinct peak at 14 (12) LT over an inland (a coastal) station. Although a 2 h shift is observed in the time of maximum mean ABL height between the stations, shifts

longer than 2 h are observed on some days. 2) The time variation of ABL is quite pronounced over both the stations. Relatively, the diurnal range of ABL height is small over the coastal station. 3) Further, the day-to-day variability of ABL height during the collapse stage is quite large, as evidenced by the large error bars during the afternoon period in both regions. 4) As expected, the mean ABL height is lower over the coastal station (~1.65 km) than over inland station (~1.95 km) throughout the day. The ABL height difference between the stations is maximum during the afternoon period, mainly due to the difference in the growth of ABL height and the delay in the collapse time of ABL between the stations. 5) Interestingly, the noon-time SNR (σ) is found to be higher (lower) over the coastal station than over inland station. It is somewhat surprising given that the inland region is characterized by strong turbulence, one one would expect high SNR over coastal region. Possibly, the prevalence of humid air (*Mohan and Rao, 2012*) and humidity gradients, important for radar backscatter in the ABL, over the coastal region might have enhanced the SNR.

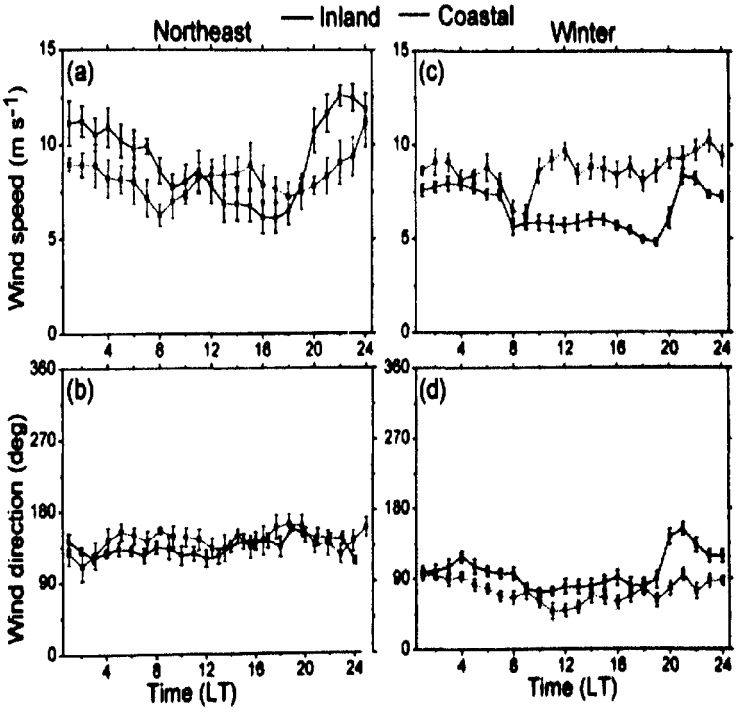

Figure 6.4: Temporal variation of mean low-level winds (below 1.5 km) obtained by WPRs (a & c) wind speed (b & d) wind direction. The mean is taken over 27 (26) and 30 (30) days for northeast (winter) seasons at inland and coastal station, respectively.

In order to understand the differences in local circulation, if any exist, between the stations, temporal variation of mean winds retrieved from both WPRs (mean is taken over all the days in the season and hourly winds below 1.5 km) is presented in Figure 6.4. The time variation of wind speed is complex during the northeast monsoon season and also distinct between the two stations. The wind maximum is observed during the late night over Gadanki, however, a double peak is observed over Kalpakkam. Along with mid-night peak, an afternoon peak is also observed, although the intensity of the afternoon peak is relatively weak. Nevertheless, there is not much variation (statistically insignificant) is seen in the wind direction at both stations (remained mostly easterly-southeasterly) and also between the stations. The diurnal pattern remained the same during the winter, but the magnitude of variation is relatively small. The time of maximum wind also shifts a few hours from that of seen during northeast monsoon.

The major forcing factors that could be responsible for the observed ABL variations between the stations are discussed briefly. The wind direction remained nearly the same over the two stations during both monsoon seasons even within 1.5 km. It suggests that the observed differences are not due to the differences in the synoptic forcing or local circulations. The observed variations are somewhat similar (differences in ABL height and its evolution) to those reported in Chapter 3, i.e., between wet and dry spells of the monsoon. The differences in surface forcing governed by soil moisture are found to be responsible for the observation variations between the spells. Note that the buoyancy flux strongly depends on surface condition, including soil moisture (*Zhou and Geerts, 2013*). The soil moisture decreases surface albedo and thus increases the net radiation (positive feedback). A reduction in incoming solar radiation at the surface or higher soil moisture content reduces the sensible heat flux, boundary layer entrainment rates, and leads to relatively shallower mixed layers (*Findell and Eltahir, 2003*). The soil moisture measurements at both locations were collected to examine whether or not the soil moisture explains the observed variations? Figure 6.5 depicts the distribution of soil moisture at 30 cm depth for both stations during the observational period. The soil moisture is higher at the coastal station than at inland station by 0.25 m^3 m^{-3} (average soil moisture is 0.42 m^3 m^{-3} at Kalpakkam and 0.17 m^3 m^{-3} at Gadanki). It shows that soil moisture over coastal region is almost 200-250% greater than inland region. The variability of the soil moisture is also higher at inland station than at coastal station, as evidenced by the wider boxplot at Gadanki. The narrow soil moisture distribution at Kalpakkam indicates that the soil moisture is not only high but such high

values persist throughout the observational period. This abundant soil moisture at the coastal station converts major portion of the net radiation into latent heat flux, rather than sensible heat flux (Chapter 3), resulting into shallow ABL. Also, as shown in Chapter 3, it delays the rapid growth of the ABL by 1-3 h, as observed in Figures 6.2 and 6.3.

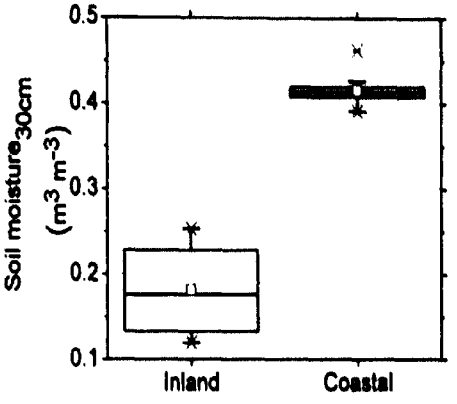

Figure 6.5: Distribution of soil moisture (depth of 30 cm) between an inland station and a coastal station during the observational period.

6.4. Differences in afternoon transition between inland and coastal stations

Complete description of the methodology adopted for the identification of AT and the variation of surface and radar attributes during the transition at Gadanki are given in Chapter 4. The time at which SNR (σ) decreases by > 1 dB (> 0.1 m s^{-1}) in 30 min is considered as the start time of the AT for that state variable. Note that the above thresholds should hold good for at least an hour from the start time of the transition. Also, all the above conditions are checked only in the data during 15:00–20:00 LT. To understand the vertical variability of transition, five representative levels are chosen (600, 900, 1200, 1500, 1800 m). To reduce random fluctuations due to noise, the profiler attributes (SNR, σ) are smoothed over both in time (10 min) and height (300 m on the chosen height). The distributions of start time AT (from profiler measurements) as identified by different state variables (SNR, σ) with respect to time of sunset over the two stations are shown in Figure 6.6 (where $Trans_{sunset}$ is referred to as (= start time of the AT-time of sunset)).

From Figure 6.6, one can see some similarities and some differences in the distribution of AT between the stations. At both sites, the start time of AT depicts height variation. It is strikingly apparent that the start time of AT is first seen at higher altitude of 1800 m (~2 - 2½ h)

before the time of sunset. There is a gradual delay in the start time of AT with decreasing altitude, following a top-to-bottom evolution at both the stations. Possible reasons for the top-to-bottom-evolution in the start time of AT are discussed in Chapter 4. The reduction in (surface) thermals strength and an increase in entrainment ratio together play a role in the evolution of AT.

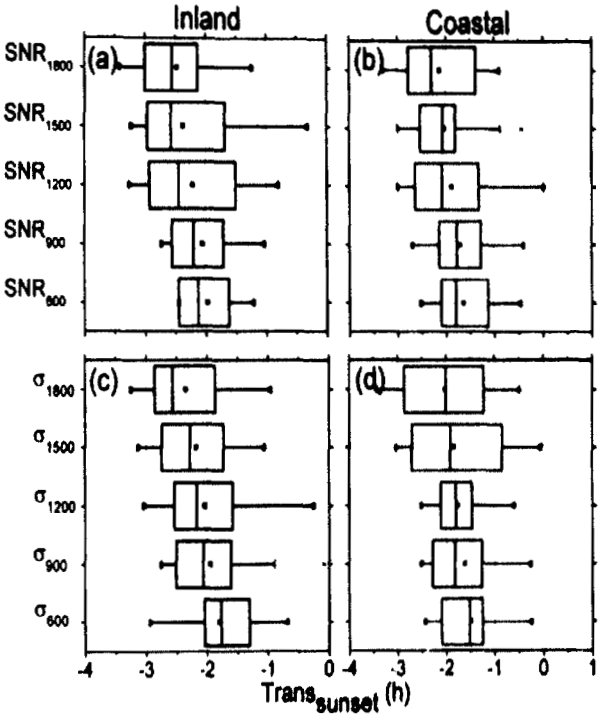

Figure 6.6: Top-to-bottom evolution of start time of AT with reference to the time of sunset, obtained from profiler-derived SNR (a & b) and σ (c & d) at an inland (left panels) and a coastal station (right panels), respectively.

The major difference in the start time of AT between the two stations is the observed delay at the coastal station at all heights. Clearly, the start time of AT is delayed at the coastal station by 20-30 min at all heights. Both attributes show this feature. The delayed AT at the coastal station is probably associated with the availability of more moisture in the air and surface. The greater heat capacity of water doesn't allow the temperature to decay rapidly at coastal station. Moreover, the turbulence is also weak over the coastal station. Therefore, large temporal gradients in radar attributes may not be present, making the identification of the exact start time of AT difficult. Since, the methodology and the thresholds used for the identification of the start time of AT is same at both stations, it is possible that the algorithm identifies the start

time of AT with some time delay at coastal stations. This is in contrast to the cross-over times of sensible heat flux during the transition at drier and wet regions reported by *Sastre et al. (2015)*. They noted that the cross-over time of sensible heat flux occurs first in wet regions. Though they attributed it to the humidity, it is not clear from their results that the observed variation is due to the difference in the degree of wetness between the stations or local circulation (the topography around the wet region is quite complex, while the dry region is homogeneous and flat). It, therefore, warrants a detailed study in future to better understand the differences in the start time of AT and the causative mechanisms.

6.5. Differences in post-sunset turbulence between inland and coastal stations

The intensity of turbulence and its persistence in the nocturnal boundary layer depends on several triggering sources, such as gravity waves, microfronts and density currents (*Sun et al., 2004; Mahrt 2010; Bonin et al., 2015* and references therein). But the turbulence generated by the above processes is sporadic in nature and relatively weak in intensity (compared to the daytime convective-driven turbulence). A few exceptions to this general behavior exist, as discussed in Chapter 5. At Gadanki, enhanced SNR and spectral widths are seen few hours after the sunset and the intensity of both SNR and spectral widths is high, in fact higher than that of seen during the day. These enhanced episodes of turbulence are referred to here as PSTs. The characteristic differences in PSTs between inland and coastal stations are discussed here.

The methodology for identifying the start time of PST and its duration is described briefly in section 5.2. The time at which the spectral width at the chosen level increases (decreases) by $\geq$ ($\leq$) 0.2 m s^{-1} in 30 min is considered as the start (end) time of PST. Similar to the analysis of AT, 5 levels are chosen (600, 900, 1200, 1500, 1800 m) for understanding its height variation and smoothed the data in both height (300 m on the chosen height) and time (10 min) to reduce random fluctuations, caused by the noise. Note that all these thresholds should hold good for at least an half-an-hour during the start and end time of PST.

Table 6.2 shows the occurrence statistics of PSTs at different altitudes over inland and coastal stations. Several interesting features can be noted from the table. 1) Clearly, the PSTs are not a rare phenomenon, rather occurs frequently (~50% of total days). 2) The omnipresence of PSTs not only limited to inland stations like Gadanki (Chapter 5), but extends to coastal stations also. 3) The occurrence of PST shows height dependency with relatively higher occurrence (> 60%

in the height region 1500-1800 m) and lower occurrence (< 50% in the height region 600 m). 4) The occurrence statistics reveal that they occur more frequently over inland stations than coastal stations. Of course, the difference in the occurrence of PSTs is small (~5-8% at all levels).

Table 6.2: Occurrence statistics of PST at different altitudes over Gadanki and Kalpakkam.

Height (m)	% of occurrence	
	Inland (Gadanki)	Coastal (Kalpakkam)
600	48.65	43.29
900	57.51	50.74
1200	59.52	52.91
1500	60.73	54.51
1800	62.45	57.74

The vertical variation of distributions of start time of PST (with reference the time of sunset) and the duration of PST (identified from temporal variation of σ) at Gadanki and Kalpakkam is shown in Figure 6.7. The indices are defined as PST_{sunset} = start time of PST - time of sunset and duration of PST = end time of PST - start time of PST. There exist some similarities in both PST_{sunset} and duration of PST at inland and coastal stations. 1) The start time of PST shows distinct vertical variability with progressive delay with height. 2) In contrast to the start time of AT, the PST start time follows bottom-to-top evolution. 3) PSTs mostly occur (the start time of PSTs) within 2 h after the sunset, i.e., within the AT period. 4) Once occurred, it persists for longer period and the duration also shows height dependency with longer persistency at higher altitudes. 5) The progressive delay in the start time of PST with altitude and increasing duration to higher altitudes suggests that the PSTs have a tilted plume structure.

Two major differences exist in the characteristics of PST between inland and coastal stations. 1) The start time of PST is delayed over inland station by 15-20 min. at all heights. For example, the mean start time of PST at 600 m is 1 h 5 min. after the time of sunset at coastal station, whereas it is 1 h 25 min at inland station. 2) Though the duration of PST is nearly equal at inland and coastal stations, but the day-to-day variability is quite large over inland station compared to that of coastal station. The PSTs persisted for whole night on some days over inland station (can be seen in Figure 6.1).

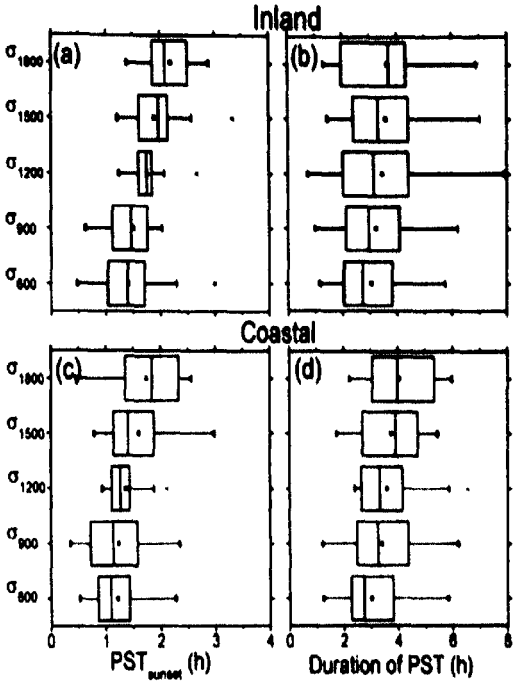

Figure 6.7: Bottom-to-top evolution of (a & c) start time of PST and (b & d) duration of PST between inland and coastal stations in top and bottom panels, respectively.

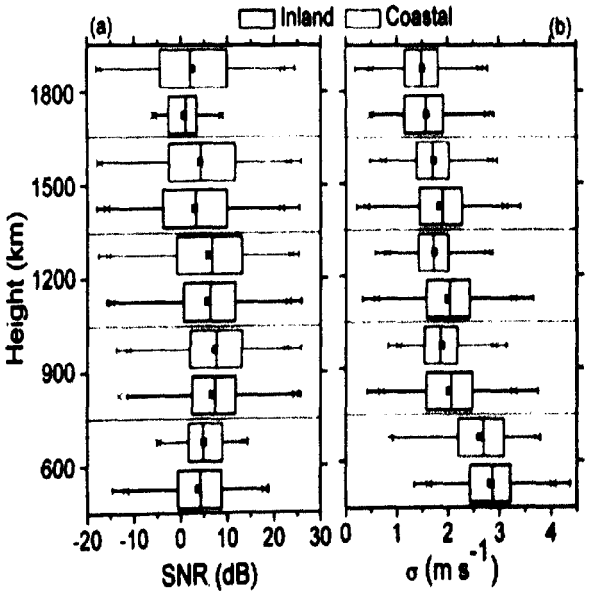

Figure 6.8: Vertical variation of distributions of SNR (left panel) and σ (right panel) obtained during the PST period between inland and coastal stations.

Figure 6.8 depicts the intensity of PSTs in terms of radar attributes (SNR and σ) as a function of height at inland and coastal stations. Though larger values of SNR are observed at the coastal station during the day time (Figure 6.3), the SNR is nearly equal during the PST period over the two stations. In contrast, the turbulence intensity is stronger over inland station than over coastal station at all heights.

6.6. Conclusions

The similarities and differences in the structure and evolution of ABL, on the behavior of AT and characteristics of PST over two diverse regions over southeast India are studied using measurements from an intense observational campaign. Two UHF wind profilers and co-located sub-surface measurements are utilized to understand the impact of surface conditions (soil moisture) on ABL characteristics. The important conclusions drawn from the present study are listed below.

1. The ABL is not only shallower at coastal station but its rapid growth is delayed by 1-2 h.
2. The time at which ABL reaches its maximum height in a day is different at different stations, i.e., 1.95 km at 14 LT over an inland station and 1.65 km at 12 LT over a coastal station. The diurnal range of ABL height is also small at the coastal station.
3. Larger SNR and smaller spectral width values are seen during the noon (11-13 LT), when thermals are very active and ABL reaches its maximum height, at coastal station than at inland station.
4. The shallow and delayed ABL growth over the coastal station is mainly due to the weak sensible heat flux governed by abundant soil moisture. Abundance of soil-moisture (nearly 2.5 times higher at the coastal station than at inland station) at the coastal station converts most of the net radiation into latent heat flux, rather than sensible heat flux and thereby reducing the height of the ABL and also delays the rapid growth of ABL.
5. On average, the signature of the AT is identified by SNR and σ are at the same time, 120-160 min prior to the time of sunset (at different levels) over the inland station, but this signature of the AT is delayed by nearly 20-30 min (150-180 min prior to the time of sunset) at the coastal station.

6. The top-to-bottom evolution of the start time of AT observed at Gadanki (Chapter 4) appears to be a common feature at all the stations, as it seen even at the coastal station (Kalpakkam).

7. The PSTs are omnipresent as they occur on nearly 50% of the days. Also, the occurrence shows height dependency with higher occurrence at higher altitudes. The occurrence of PST is relatively higher at inland station than at coastal station at all chosen levels.

8. The start time of PST shows a height variation with progressive delay with altitude, following bottom-to-top evolution. The duration of PST increases with altitude. Together, they appear like a tilted plume.